Universidad de los Andes

Physics department

Measurement and Characterization of Granulation Pattern in the IAG Solar Flux Spectrum

BSc Physics Final Project

Author:

Claudia Alejandra Cuellar Nieto

Advisor:

Benjamin Oostra Vannoppen

Nov 2025

Abstract

Hello, this is my work :D

Acknowledgements

Thanks :b

Contents

List of Figures

Chapter 1

Introduction: The Sun's granulation pattern

For decades, the solar spectrum has served as the fundamental reference point for spectroscopic analysis and characterization. As our nearest star, the Sun has enabled comprehensive studies of stellar composition. However, advances in optical instrumentation have recently revealed previously undetected spectral details, providing new insights into even the most basic solar properties from dynamics to surface geometry. One of this advances is the granulation pattern due to convection motion, which is revealed by three fundamental signatures of its hydrodynamics: Line broadening, line profile bisector asymmetry, and line-depth dependence of the convective blueshift.

Inspired by Gray's foundational research [3], this project seeks to extract the granulation pattern from the IAG Solar Flux Atlas to calculate relative velocities and perform detailed analysis. A parallel focus will investigate the chromatic dependence detected in absorption line profiles (the third signature of convection), which currently obscures the universality of the pattern.

1.1 Convective motion

The stellar spectrum serves as astronomy's primary source of information, particularly regarding a star's composition and relative velocity. However, convective motions in the stellar photosphere complicate spectral interpretation by inducing differential velocities in individual spectral lines. Specifically, fluid movements caused by density variations from temperature fluctuations in the Sun's outermost layer modify the spectrum, causing each spectral line to display distinct relative velocities as we can relate to different research [4, 5, 3, 6]. Persistent convective motion generates a granular structure in solar photospheric images. One of the first person to discover the pattern was Janssen in 1885, who detected a granulation movement in the photosphere. Lately, in 1901 Plasketts associated this pattern with te same of convective cells in Bernard's experiment [7]. Where fluids heated from bellow representing hot rising gas elements convecting heat to surface. This characteristic configuration gives the name *granulation* to all observable signs of the convection.

1.2 Solar granulation pattern

A plot of Doppler shift against line depth is called *Granulation Pattern*; it shows that weaker lines are more blueshifted. When the Sun pushes material up through its outer layer, the spectrum exhibits a blueshift. As this material subsequently cools and falls back through the atmosphere, it produces a redshift, but emits less light, making the blueshift dominant. This phenomenon has been particularly documented by David Gray, whose work has significantly improved the precision of stellar radial velocity measurements. This improvement stems primarily from Gray's observation that granulation patterns in stars resemble solar patterns, differing only by a scaling factor. These findings are particularly significant given the considerable challenges in obtaining such parameters for other stars, which are affected by spectral noise, stellar proper motions, and relative velocity uncertainties [3]. Furthermore, analysis of solar granulation patterns contributes to the understanding and validation of photospheric hydrodynamic mod-

els [4]. Such analysis enables improved calibration when testing dynamic atmospheric models.

1.2.1 The three signatures of convection

Due to convection motion, there's three distinct granulation signatures can be identified in stellar spectra: Line broadening, line profile bisector asymmetry, and line-depth dependent shifts in absorption lines [8]. The third signature exhibits a correlation between line depth and wavelength shift[3], for which neutral iron lines (Fe I) serve as optimal calibration references due to their high abundance, minimal thermal broadening and limited isotopic variation. This approach offers the additional advantage of deriving natural wavelengths from a single source, thereby eliminating potential discrepancies.
On the way of trating th Sun as any other star, which does not have the proximity for spectra study, we search for obtain the most accurate and precise granulation pattern. Which is posible if we take the most accurate and precise solar atlas.

1.3 IAG Solar Flux Atlas

In 2016, Reiners et al.[6] published the unprecedented precision *Institut für Astrophysik Göttingen (IAG)* Solar Flux Atlas obtained with the FTS *Fourier Transform Spectrograph*, simultaneously reporting convective blueshifts for a sample of neutral iron lines. This atlas provides highly precise and accurate data, with radial velocity uncertainties on the order of $\pm 10 m/s$ across the wavelength range of 4050 to 10650 $\mathring{A}$. In contrast to other FTS atlases, the entire visible wavelength range was observed simultaneously using only one spectrograph setting[6].
In 2016, the resulting granulation pattern appeared notably scattered and noisy, attributable to the rudimentary line position measurement methodology employed, and the poorly curated line selection, which included numerous blended features, outdated wavelength references and incomplete spectral coverage. The exceptional quality of the IAG spectrum enables more accurate determination of convective blue-shifts when

analyzed through refined methods.

1.4 IAG Spatially Resolved Quiet Sun Atlas

In 2023, Ellwarth et al.[9] observed and published the *Institut für Astrophysik Göttingen (IAG)* Spatially Resolved Quiet Sun Atlas obtained with the FTS *Fourier Transform Spectrograph*. This atlas has the advantage of use observations from the disc center ($\mu = 1.0$) towards the solar limb ($\mu = 0$), where $\mu = \cos(\theta)$. The research had the objective of study the blueshift exhibits variations from the disc centre to the solar limb due to differing projection angles onto the solar atmosphere.

Our principal objective is to establish a characterization of the granulation pattern by treating the Sun as any other star. This approach allows us to develop methods that can be directly scaled and applied to other solar-type stars. However, to accurately analyze relative velocities and dynamics, we must account for insights that can only be corrected using the Spatially Resolved Quiet Sun Atlas.

1.5 Motivation

During the first semester of 2025, physics student on the Universidad de los Andes Manuel Fuentes implemented these improvements in his computational project, focusing specifically on the visible spectral range $4050 - 10650$ $\mathring{A}$. By developing enhanced measurement techniques and employing a carefully curated line list that fully covers the IAG-VIS range with updated wavelength references [10], Fuentes achieved significantly sharper granulation patterns compared to previous analyses. This optimized approach demonstrates how proper line selection and modern wavelength standards can extract more reliable convective signatures from high-quality solar spectra.

With professor Benjamin, we continue with a measurement of granulation pattern taking into account the near infrared range. This region contains spectral lines originating from deeper layers of the solar photosphere, which are consequently weaker. These lines

represent a rich source of valuable information [11], though they require adapting the measurement methodology. Furthermore, we start a characterization of solar dynamics and line asymmetries based on granulation pattern observations.

By addressing these challenges, we aim to achieve two key outcomes: A robust characterization of solar granulation pattern and insights into the photosphere's geometry. These efforts are guided by the central research question: What are the direct consequences of solar dynamics on its spectrum?

Chapter 2

Literature Review: Convective movement in the Sun

As previously mentioned, David Gray[3, 8] has significantly advanced the study of granulation patterns in the solar photosphere, with a particular focus on measuring their associated relative velocities with high precision. These developments have enabled more accurate characterizations of other stars by extrapolating the physical principles observed in the Sun. This chapter explores the three signatures of convective motion in the Sun photosphere, and how this reveal the hydrodynamic on this outermost layer. Furthermore, is given the point of view of different authors respect the reasons behind the chromodependece on the granulation patterns.

2.1 The solar interior and the solar outer atmosphere

The Sun is classified as a yellow dwarf star of spectral type G2V, title achieved for a big amount of hot hydrogen (ionised H in 90 percent) and helium (in 10 percent). What makes this star really unique is his proximity to earth and the facility to study from the planet with precision. In general, the Sun is divided in two fundamental parts: The

solar interior and the solar outer atmosphere.

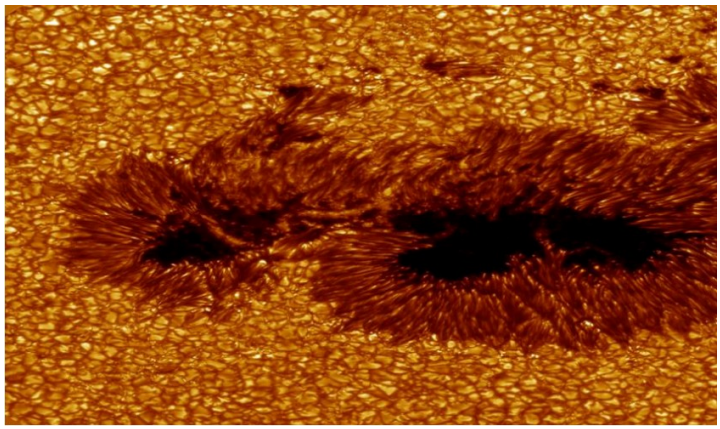

Figure 2.1: The interior structure of the Sun. The convection zone is the responsible by the general movement that characterize the third signature.

As shown in the figure 2.1 the overall structure of the solar interior is core, radiative and convective zone. Across then the density and temperature falls significantly, as the energy is slowly transferred outwards by radiative diffusion. Some models of the interior structure give a core temperature of $1.6 \times 10^7 K$ and density to $1.6 \times 10^5 Kg/m^3$, high enough for thermonuclear reactions and remains the central material in plasma like a gigantic atomic reactor. This characteristic allow the collisions, absorptions and reemisions of photons that made this zone opaque. In consequence, there exists an increase of the wavelength from high-energy gamma rays to visible ligth.

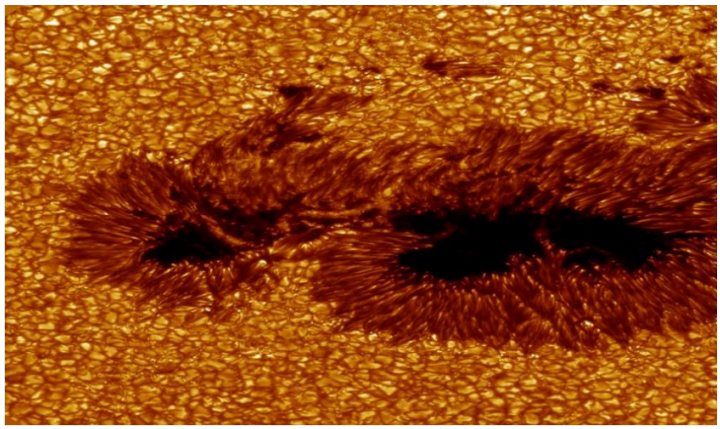

Figure 2.2: The outer atmosphere of the zone. The photosphere is the layer of the sun where is visible the convection motion.

On the other hand, the figure 2.2 shown the overall structure of the solar outer atmosphere which consist in photosphere, chromosphere and corona. In this part the density decreases rather rapidly with height above solar surface, and the temperature decrease to 4300 K for then rises through the transition region. Thereafter, the temperautre falls slowly expanding outwards as the solar wind. From this the photosphere emits a continuous spectrum with superimposed dark absorption lines where most of this wavelengths are absorbed by the chromosphere [12].
The target layers of this study are the conevction zone and the photosphere, which will focus in further sections.

2.2 The Solar Convection Zone

This is a zone ubicated at one solar radius. In this zone the temperature gradient is great for the material to stay in static equilibrium, and is where the magnetic field is generated[12]. Until 1885, when Janssen took a photography of the granules in the photospere and Plasketts relationed these granules with the Bernard laboratory measurements of fluids convection, they took into account the dynamics of the layers in the Sun [7].

2.2.1 The convection movement

In 1930 Unsold pointed out that the layers below the photosphere should be convective unstable. In 1936 Plasketts sugested that granules looked similar to the pattern of convective cells found in Bernards experiments. This statement are based on fluids heated from below representing hot rising gas elements convecting heat to surface. This last is caused by the Janssen observations in 1885, when take a photography of photospere showing pores and granulation [7]. So, we see the photospheric granules as convective cells. Have been shown to be influenced more by surface tension in the shallow near layers than by the bouyancy forces that drive free convection. Solar convection occurs in a highly compresible, stratified gas[7]. When a liquid layer is heated from below, convection iniciatilly sets in a 2d, horizontal, parallel rolls. The existence of a 3d convection pattern of convection cells that is static is limited to fluids whose viscosity ν is high compared to their thermal conductivity κ (the ratio of this two is the Prandtl number P). Fluids with $P \approx 1$ in Laboratory show little evidence of steady 3D convection, an increase of the gradient temperature leads to a turbulent flow pattern. But at te photosphere with $P \approx 10^{-9}$ we expect to find turbulent behavior in the granulation if the temperture gradient is sufficient to drive free convection at the observed velocities and horizontal temperature differences[7].

2.2.2 Dynamics of solar convection

To determine the conditions under which we expect convection we suppose that a small elements of mass m stay in radiative equilibrium has P, ρ, T, the same as its surroundings at radial distance r from the center of the star. Onset of convection: If T is increased to a value T', the gas in this element will expand rapidly to achieve a new pressure equilibrium with its surroundings. The lower-density gas will experience a bouyancy force, which will cause it to rise. The bouyancy force will disappear when the density has dropped to the same value as that of its new surroundings after an element has traveled a distance l. Let be T_1' the new temperature and that of its surroundings T_1 (l

is small) So

$$T_1 = T + \left(\frac{dT}{dr}\right)_R lT_1' = T' + \left(\frac{dT}{dr}\right)_{ad} l \tag{2.1}$$

Where the ad is for adiabatic gradient and R is for radiative gradients. Since we have assumed radiative equilibrium, the R denotes the gradient present in the stellar atmosphere. Two conditions can arise from here:

First, $T_1' > T_1$ what is like $\Delta T > 0$ so equation () follows.

$$-\left(\frac{dT}{dr}\right)_R > \left(\frac{dT}{dr}\right)_{ad} \tag{2.2}$$

This is the element continues to expand further and rise. So, convection pattern is established and the radiative gradient is unstable.

The other condition, as it be, the element begins to contract, becomes heavier, and begins to move down to its original position. The radiative gradient is stable, and a displacement element will undergo oscillation.

2.2.3 The Schwarzchild Condition

Convection will tend to take over as the energy transport mechanism wherever the radiative gradient temperature becomes large due to the large local opacity or strong local energy generation. So, convection can set when opacity rises very rapidly due to increasing population of n=3 level of hydrogen, and when γ is lowered by ionization.

The equation (2.7) stablish the criterion for presence of convection. As the presence of convection reduces the temperature gradient from the higher value it would have assumed under radiative transport alone to the essentially adiabatic value [7].

2.2.4 The parcel argument

From the core, He nuclei is built from H nuclei in the proton-proton cycle as say equation(2.3).

$$4^1H \rightarrow^4 He + 2e^+ + 2\nu + 26.7MeV \tag{2.3}$$

Where from the H nuclei is liberated an considerable amount of high frecuency $\gamma-$rays ($26.7MeV$) and the energy of 2 neutrinos (0.5MeV). The strong Coulumb repulsion

between positevily charged nuclei increases as the product of their nuclear charges, so only lightest elements will have appreciable reaction probabilities [7]. As the electrons recombine with others particles the photons can be absorbed more easily. With this, decrease the radiative conducity and increases the temperature gradient with the opacity. In the boundary of radiative zone the temperautre is drecreasing rapidly, so it begins a convective instability and beyond a convective trubulence. When reaches the low photosphere, some radiation scape from the sun and the material returns to the convective stability [12].

The onset of instability when the vertical temperautre gradient is too large is explained by the parcel argument and the Schwarzchild condition. Consider a vertical stratified plasma in hydrostatic equilibrium with pressure ($P(r)$); density ($\rho(r)$); and temperature ($T(r)$). Now suposse an elementary parcel of the material is displaced so slowly that remains in horizontal pressure equilibrium. Then the parcel will feel a bouyancy force and continue raise if $\delta\rho_i < \delta\rho$. By the ideal gas law, the density changes need to follow the equation(2.4).

$$\frac{\delta P_i}{P} = \frac{\delta\rho_i}{\rho} + \frac{\delta T_i}{T} \tag{2.4}$$

Remains the same for the final state. But for static equilibrium, the conditions (2.5) are gonna make the parcel unstable and the fluid will continue raising.

$$-\frac{dT_i}{dr} > \frac{dT}{dr} \text{and} \delta T_i < -\delta T \tag{2.5}$$

If the motion is adiabatic there is no heat exchange with surroundings. So the rate between the density and pressure is constante, what generates a limit in the adiabatic temperature gradient (see equation (2.6)).

$$\frac{dT_i}{dr} = \frac{\gamma - 1}{\gamma}\left(\frac{GM_{\odot}m}{r^2 k_B}\right) \tag{2.6}$$

Where k_B refers to Boltzman constant, and γ the degree freedom of the fluid. With this limit the criterion for conevctive inestability becomes the equation (2.7).

$$-\frac{dT}{dr} > \frac{\gamma - 1}{\gamma}\left(\frac{GM_{\odot}m}{r^2 k_B}\right) \tag{2.7}$$

When H and He nuclei become ionised, they can absorb energy by more degrees of freedom; this decreases the value of γ and the adiabatic temperature gradient, which makes convection easier. It has been sugested that granulation are driven by the ionization of H and He, and have scales comparable with the depths at wihich processes take place[12]. From surface observations the convection appears to be domination by cells: Granules, mesogranules, supergranules and giant cells. These granules can perturbe the angular momentum of the sun and the flow patterns in this zone.

2.2.5 Contributions on angular momentum

The pronounced differential rotation with latitude observed at he photosphere seems to be the result of convective flows driven radially by the bouyancy force and deflected horizontally by the coriolis force due to solar rotation (term of $2\rho\vec{\omega} \times \vec{v}$). Is dificult to datermine wheter the coriollis effects acts on slow global scale axysimmetrical circulations in the meridional plane, on intermediate scale eddies, or on a hierarchy of small eddies [7]. There are two types of contribution on angular momentum. The first contribution is the meridian circulation. Occurs if axysimmetric meridional circulation are present. Movement of fluids in a vertical plane. In the absence of any other angular momentum transport, a circulation in either sense will tend to spin up the poles and the interior because the fluid carries angular momentum. These regions will be spin up (activating) until the flux of ωr^2 is equal both radius and latitude [7].

The second contribution is the reynolds stresses. These process tends to enforce solid body rotation, then the meridional circulation drive an equatorial aceleration. The reason is that for equal velocity in the meridional plane, the flux of angular momentum per unit mass across the dashed line will be larger toward the equator than away from it. This mechanism depends on the existence of nonaxisymetric convective motions. Because net fluxes of angular momentum in latitudinal or radials directions are produced without requering a net mass flux. They play an important role in the dynamics of turbulent fluids [7].

Neither buoyancy forces, which are strictly radial, nor presure gradients, which must

average to zero around the solar circumference, can themselves influences the suns axysimetric rotation profile[7].

2.3 The Solar Photosphere

Since 1874, when Langley gives a detailed description of granulation on the photosphere, the astronomers have been studied different motions and reactions across the layers [12]. Is an extremely thin visible surface layer, is only 100km thick and centered in the region where $T = 5000K$. In high resolution spectrograph shows a granular struture and a filme shows these brigth granules to be in continual motion. These granules represents the top of convective cells that are overshooting the upper convection zone. There are composed by hot, rising and horizontally outflowing plasma rather than cooling material. This is the region where magnetic flux is concentrated [12].

The solar atmosphere is highly inhomogeneous and turbulent but we can take a start point. This is named Harvard-smithsonian reference atmosphere. It cero level is taken as the point where optical depth at a $\lambda = 5000\mathring{A}$ is equal to one.

For the deeper analysis we carried out is better to see separated the static and dynamic photosphere.

2.3.1 Static photosphere: Limb darkening phenomenon

The photosphere intensity falls off towards the limb, cause the temperature decrease of the higher layers as we look nearer the limb. The analysis of this effect provides a direct technique for determining the photosphere temperature structure with depth. This effect drecreases with increasing wavelength, the disk intensity profile becomes more squared at infrared. Since the limb darkening is caused by the temperature gradient we might to expect it to disappear in the infrared or ultraviolet where we observe layers around the $T_{\min}$ [7].

2.3.2 Dynamic photosphere. The C-curved profile bisector.

There exists a heigth dependence of the granular velocities. The velocity of an upward moving granule decays much less rapidly than its excess brigthness. The granular material is dark when observed in Fraunhofer lines formed high in the photosphere. So the material is cooler caused by its rapid expansion. Changes in the granulation structure, contrast and velocity field around the spots and network have been infered indirectly from observations of Fraunhofer line profile shapes. The result is characteristically C-Curved profile bisector [7]. The process of the creation in this c-curved profile bisector is listed before:

- The line profile near its mid-depth portion is formed in the most rapidly upflowing bright material. Blueshifted.
- The deepest portion of the line core is formed higher in the decelerated upflow. Less Blueshifted.
- The line wings, where the opacity is least, tend to be formed deepest in the cool. Redshifted.

The bisectors tend to be less c-curved near solar activity maximum that at minimum. Near activity maximum the higher packing density of magnetic flux tubes will tend to disrupt granular convection[7].

2.4 Solar granulation pattern

When observing images of the solar photosphere, a distinct pattern of bright and dark regions with dynamic behavior becomes apparent, where individual areas continuously emerge and disappear (see figure 2.3). This phenomenon is known as granulation, and each individual region—spanning approximately 700 km in size and lasting between five to ten minutes—is referred to as a granule.

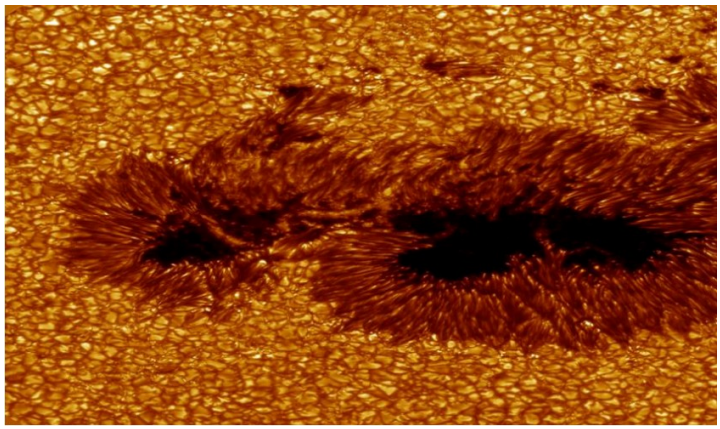

Figure 2.3: A view of the granulation pattern on the Sun's surface. The central regions exhibit blueshifts while the edges display redshifts. Image taken from [1]

Solar granulation arises due to the "eruption" of the convective zone at the base of the photosphere [3]. Spectroscopic observations of the Sun reveal asymmetries in absorption lines caused by the motion of the solar atmosphere within granules. These asymmetries occur because some parts of these convective regions are blueshifted, while others are redshifted. The bright areas of granules correspond to regions where hot gas rises through the solar atmosphere, producing blueshifts in absorption lines. As this gas releases energy in the form of photons at the photosphere, it cools and subsequently descends, creating the darker regions of granules, which exhibit redshifts in absorption lines [13].

As we mention before, this granulation pattern arises from convective motions within the solar photosphere. These motions consist of an upward flow of matter from hotter inner layers to cooler outer regions—and vice versa. This dynamic process induces perturbations in spectral absorption lines, profile asymmetries, and depth-dependent wavelength shifts [8] known as the three signatures of convection (name given by [3]).

Is important because granultion patterns in stars resemble solar patterns, differing only by a scaling factor (see [8]). Furthermore, these analysis contributes to the understanding and radiation of photospheric hydrodynamic models [4, 3].

2.4.1 Convective Blueshift

When the Sun pushes material up through its outer layer, the spectrum exhibits a blueshift. As this material subsequently cools and falls back through the atmosphere, it produces a redshift, but emits less light, making the blueshift dominant.

Relativistic Doppler Effect

The Doppler effect is a wave phenomenon caused by the relative motion between a source and an observer, resulting in a measurable shift in the electromagnetic spectrum compared to laboratory or catalog reference values. However, in astronomical contexts—where velocities can be significant—the relativistic formulation of this effect must be applied.

The relativistic Doppler effect accounts for length contraction, as predicted by Einstein's theory of relativity. This introduces an additional correction term to the classical shift, which becomes particularly relevant in high-velocity scenarios or strong gravitational fields.

$$f_{obs} = f_{rep}\frac{\sqrt{1 - v_r/c}}{\sqrt{1 + v_r/c}} \tag{2.8}$$

As indicated in equation (2.8), the observed frequency f_{obs} corresponds to the light detected by an observer, while f_{rep} is the frequency emitted by the source, and v_r denotes its radial velocity [14].

$$z = \frac{\lambda_{obs} - \lambda_{rep}}{\lambda_{rep}} = \sqrt{\frac{1 - v_r/c}{1 + v_r/c}} - 1 \tag{2.9}$$

Since cosmic expansion dominates the universe's large-scale dynamics, the parameter z, known as redshift, was introduced. This term quantifies the relative recession of distant objects and can be expressed through the relativistic Doppler effect, as shown in equation (2.9).

2.4.2 Convective Blueshift and Relative Velocity

However, in our study, we will define this blueshift resulting from specific motions as *convective blueshifts*. This phenomenon occurs when spectral lines in stellar light, including the Sun's, appear shifted toward shorter wavelengths due to convective motions in the star's atmosphere [3]. Taking into account that most astronomical phenomena move with velocities much smaller than light, the equation (2.9) can be approximated to first order.

$$\sqrt{1 \pm v_r/c} \approx 1 \pm \frac{v_r}{2c} \quad \rightarrow \quad z \approx \frac{v_r}{c} \tag{2.10}$$

From the expression (2.10), is advantageous to reform for the equation (2.11) with the approximation of relative velocity.

$$v_r \approx c\frac{\lambda_{obs} - \lambda_{rep}}{\lambda_{rep}} \tag{2.11}$$

With this equation the calculus of relative velocity is straightforward; therefore, the perturbations in spectral absorption lines.

This phenomena is a impediment to determing true radial velocities of stars to accuracies better than a few hundred m/s. Since the strength of the convective distortions and shifts os spectral lines varies across the H-R diagram, we expect the systematic errors in radial velocities [3].

In resume is a graphic of doppler shift against line depth, it shows that weaker lines are more blueshifted.

2.5 The three signature of convective motion

With all the mentioned about convection, there are thre signatures for identified convection in the outer atmosphere for a start. In our case we are just take the sun.

2.5.1 Line broadening

Due to the limb darkening phenomen the photospheric intensity falls off toward the limb, cause the temperature decrease of the higher layers seen as we look nearer the limb [7].

This effect decreases with increasing wavelength, the disk intensity profile becomes more squared at infrared. Or as we call weaker lines.
This is measurable with the core curvature or the second derivate in the observed wavelength.

2.5.2 Line profile bisector asymmetry

As mention [5, 4] we treat with a C-curved profile bisector assymetry due to convective blueshift. So we expect a difference in the bisector slope (thir derivate relation proved in the apendix).
Absorption spectra from the solar photosphere exhibit asymmetries that may be measured using the bisector method. This technique involves tracing a line connecting the midpoints between the spectral profile's wings at different intensity levels. The phenomenon is particularly prominent in spectral lines of pure elements; for this study, we specifically focus on neutral iron lines (Fe I) due to their low sensitivity to thermal motion, and other virtues, as mention below.
The solar spectrum reveals that our star emits radiation in the visible and infrared ranges following approximately a blackbody curve. This behavior indicates the presence of a continuous opacity source across the observed electromagnetic spectrum. This continuum opacity is primarily due to H^+ ions in the photosphere, which are responsible for hydrogen's contributions to the spectral continuum. According to Kirchhoff's laws, absorption line formation requires lower temperature conditions, which are found precisely in the Sun's outermost atmospheric layers [13]. These regions not only provide the appropriate temperatures for absorption line formation but also exhibit comparatively higher opacity. Among all available spectral lines, those from neutral iron are particularly valuable for solar granulation studies due to two key characteristics: they display significant opacity and relatively low thermal broadening. These properties make Fe I lines excellent tracers of granulation patterns in the solar photosphere [2]. These asymmetries are physically significant because absorption line profiles should theoretically be symmetric under ideal conditions. Their detection directly reveals the influence of pho-

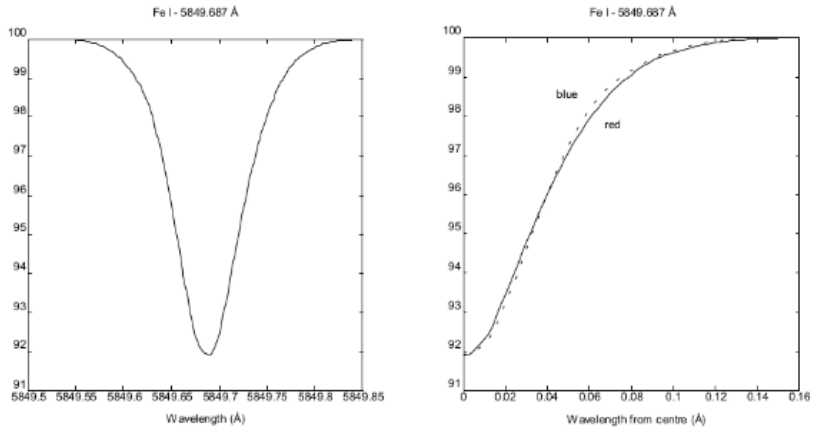

Figure 2.4: Asymmetries on an average absorption line. Can be observed the differences in intensity redshift profile. Image taken from [2]

tospheric granulation patterns. As demonstrated by Nieminen [2], the asymmetry occurs because each individual profile component contributes a distinct convective blueshift, reflecting velocity variations between atmospheric layers where convection dominates and the more stable interior regions (see figure 2.4).

Defining the base of what we recognize as the photosphere is not a trivial task, primarily due to the dependence of optical depth on wavelength. This means that the observed radiation must traverse varying densities within the solar medium, where the temperature gradient across this atmospheric layer significantly influences its propagation.

2.5.3 Line-depth dependent shifts

Many studies across the yers have detected and observed the phenomena of wavelength shifts againts the line depth, or as it is called, chromodependence in the granulation pattern. This behavior was showed to be more present in the weaker lines (less depth) which are related to infrered and violet range. However, the many studies didn´t present a general characterization of this phenomena, just describe the problem.

The article which try to stablish a "standard" curve is [15] where is presented a second grade polynomial fot to the solar granulation pattern. But, the authors just take the green range of the spectrum, avoiding the chromodependece in the weaker lines. This

motivate us to search a strong characterization and give the recipe for dealing with this phenomenon.

2.6 Teluric Absorption Lines

In the near infrared range we can denote a natural bands or groups of lines which are separated for the teluric elements, on others words, elements like oxygen and CO2 that are absorbed by the atmosphere. Tis range are invisible for the spectra, and it helps us to detected the natural bands in the near infrered curvature profile.

Chapter 3

Methodology: The blend-free list of Fe I lines

As the spectral analysis is complicated cause the convective motion, I take an computational approach leading an observational requirement to lead the research. This leading by the experience of professor Benjamin and the previous research. This research endeavor encompass both analytical and computational components. For the last part, the programming language Python and Jupyter Notebook was used. The computational aspect focus on identifying the granulation pattern within the solar spectrum by calculating relative velocities using the wavelengths of Fe I. All analysis data and code used in the process was uploaded to a GitHub repository, allowing anyone interested to reproduce the results and verify the authenticity of the conclusions presented. Moreover, proper credit will be given to all previous work from other researchers.

3.1 Methodology

We follow the methodology established in previous studies [4, 6, 9] , which utilized a selected list of Fe I lines. These lines are ideal for this calibration due to their minimal thermal broadening and reduced susceptibility to other atmospheric affectations.
The line up for the code was identify the Fe I lines in the IAG Solar Flux Atlas and the

IAG Spatially Resolved Quiet Sun Atlas using the blend-free list of Fe I lines. Second, fit a fourth-grade polynomial fit due to the c-curved line profile bisector and find the observed wavelength. Then calculate the Doppler velocity, convective blueshift and flux with the fit. Finally, find the second derivate (core curvature) and the third derivate relation (bisector slope) for the curvature in the observed wavelength. This last is develop in detail in the apendix B.

3.2 Blend-free Fe I line list

The previous methodology implemented the Nave et. al list of laboratory measured Fe I lines [10]. This list classifies lines with a quality rating (A,B,C,D) with A be the most and best quality. However, not all the listed lines are clearly present in the solar spectrum, and within the near-infrared range, many lines are severely mixed.
In collaboration with Professor Benjamin and Manuel Fuentes, we refined this list.

3.2.1 Selection method for Fe I lines

This selection method has two different approaches: Computational and visual. First, we selected only quality A lines and then performed the next filters according to the statement of having an fourth order polynomial fit for the line core.

- The coefficient of the fourth grade term need to be positive and not too small cause it denotes a curve too big. This can be for a line, specially in the infrared, cause the big cores are related to atmospheric lines.
- The difference between extreme points of the fit need to be less than the half of the distance, that is a curve and not a slope.
- The absolute difference between the wavelength observed and the one from Nave list need to be less to $0.025\mathring{A}$.

The last part was a visual inspection to discard line mixes or absent from the solar spectrum. This part was divided between porfessor Benjamin and me. I used the

visualizer (explained in detail in the apendix C) and profesor Benjamin use the great years of experience. Then I combined the list, made a check and profesor Benjamin check again. The discard part was only using the geometry of the curve and guidance of profesor Benjamin (and God). The new blend-free list improves our results, leading to cleaner graphics and characterization with less scatter in the data. Then we perform different graphics for our analysis conform we see it necesary for the characterization. In case of the IAG Spatially Resolved Quiet Sun Atlas we only use the $\mu = 1$

Chapter 4

Results and discussion: Granulation pattern and Characterization of chromodependence

Our results can be summarized in three principal aspects: Chromodependence on the granulation pattern along the line depth; a detailed view of the characteristic curvature, asymmetries, and sharpness of spectral lines and higher-quality graphs with reduced scatter.

4.1 The third signature: Chromodependence on the granulation pattern

We obtain the granulation patterns for the IAG Solar Flux Atlas for all the wavelength.

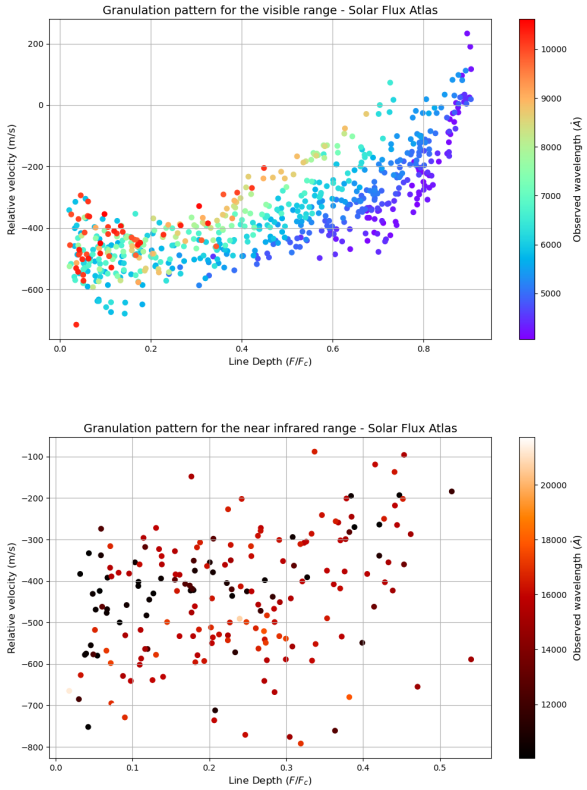

Figure 4.1: Granulation pattern for the Solar Flux Atlas.

The behavior along the line depth is according to literature, in which is clear the chromodependence. For a different try into the characterization of this behavior we try to genearte different second order polynomial fits for each color range.

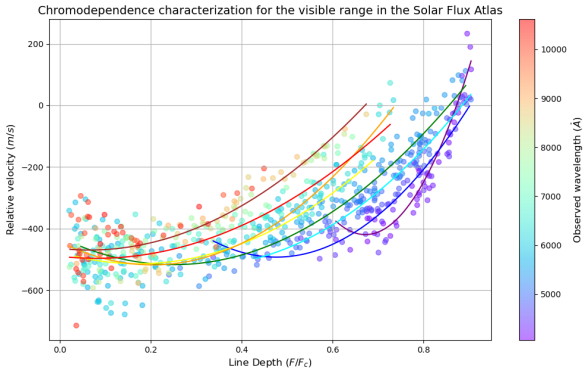

Figure 4.2: Granulation pattern for the Solar Flux Atlas with color curves.

But this is not standard. So, we performed an analysis of line depth against wavelength. Our hypothesis was: "If the chromodependence is present only in the Solar Flux Atlas, then rotation could be the cause of this phenomenon" Surprisly, we observed a chromodependence in both spectral datasets. We start taking the granulation pattern of the center disk

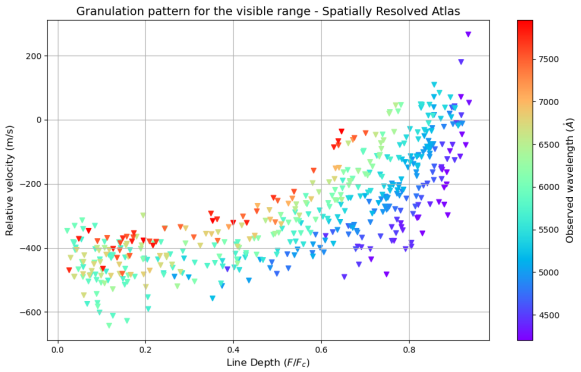

Figure 4.3: Granulation pattern for the Spatially Resolved Quiet Sun Atlas at $\mu = 1$.

This was initially unexpected because the rotation is negligible at the disc center. For the measurement of its velocity we took a 4300-5600 A range and sorted all lines from both atlases into 50 m/s velocity bins.

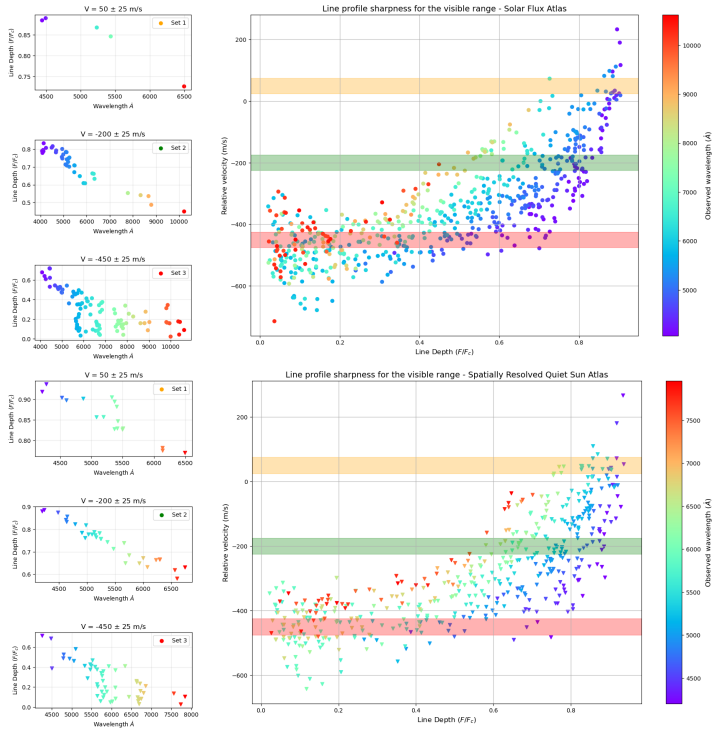

Figure 4.4: Comparision between atlases with velocity bins for the relation between wavelength and line depth.

For the measurement of rotation in the lines we made a first order polynomial fit for each one.

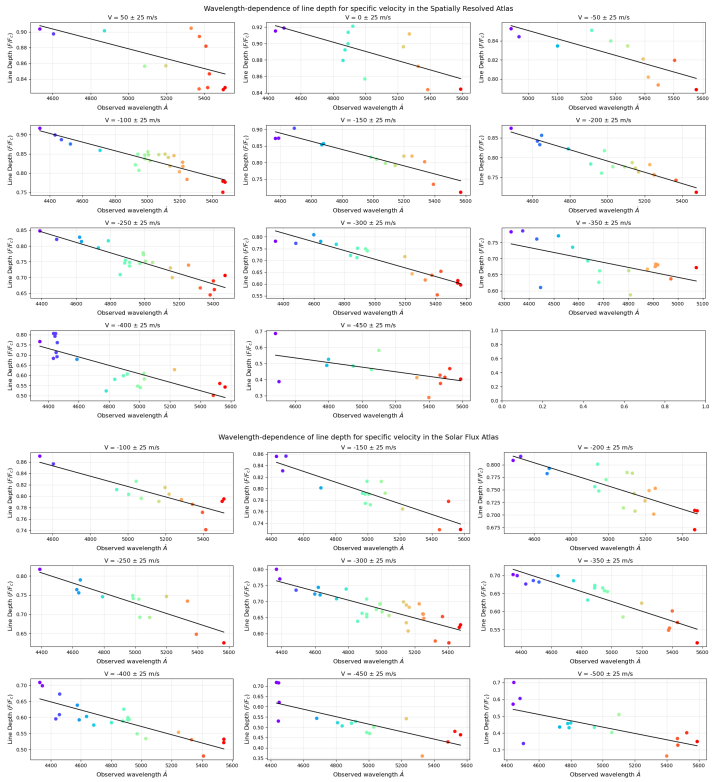

Figure 4.5: Comparision between atlases with velocity bins for the relation between wavelength and line depth. The first order fit is showed for each velocity bin.

The clue here is the value of slopes in the Spatially Resolved Atlas is greater than the Solar Flux, which contrindicates for complete the initial hypothesis. The rotation is not the cause.

4.2 The first and second signature: Detailed view of line broadening and asymmetry

We made two graphics corresponding to each signature related to the line bisector and core asymmetries. The slope of line bisector shows the behavior of the c curved line profile bisector.

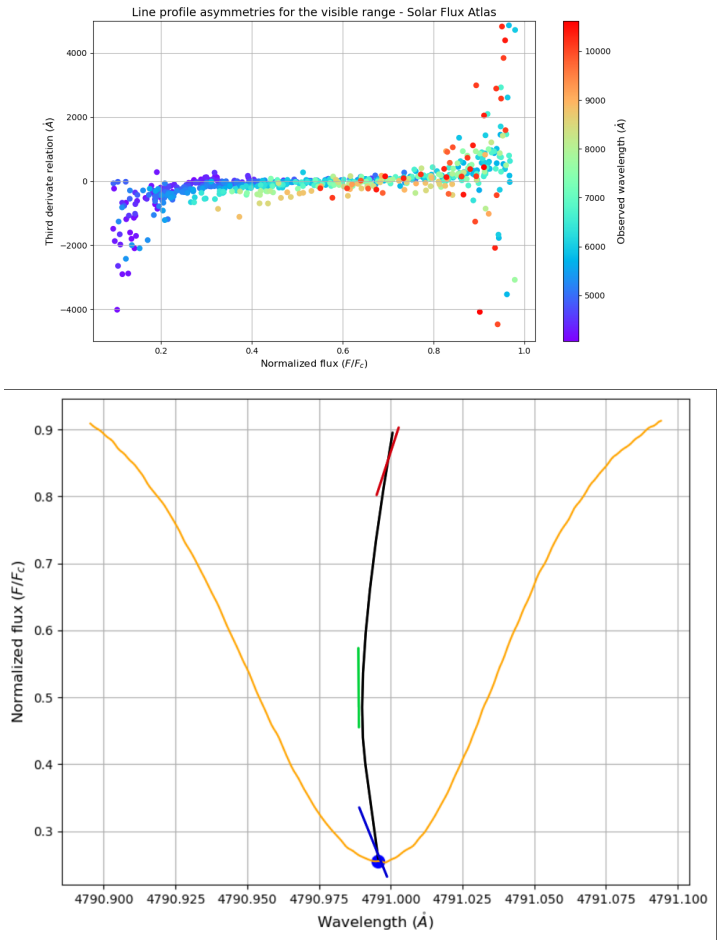

Figure 4.6: C bisector graph for slopes in ehich is clear the convection movement and how its affected in the profile.

The interesting one is the core curvature but multiplied by the squared wavelength, cause it affirms the chromodependence in the weaker lines as the literature says.

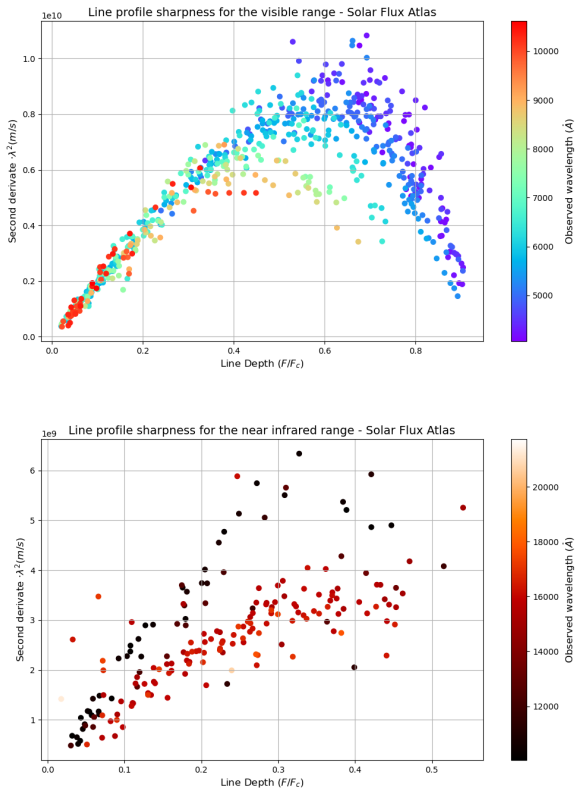

Figure 4.7: Sharpness of the core bisector in the solar flux atlas separated by range.

We can see a natural division for lines in the infrared range, which is interesting due to corresponding Teluric lines of absorption in the atmosphere. Theres is a little division in $11400A$ who separates the lines i one that follow the mean curve and others than doesnt do that.

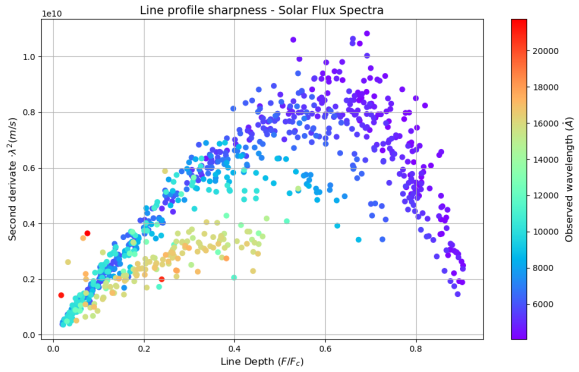

Figure 4.8: Sharpness of the core bisector in the solar flux atlas. Is clear that the infrared follow two different behavior due teluric lines.

This is the graphic which is clear that we have chromodependence in the weaker lines.

4.3 Higher quality graphs

In comparation of Ellwarth graphics, which is the study most recent, there is a better resolution in the different graphs without scattered points.

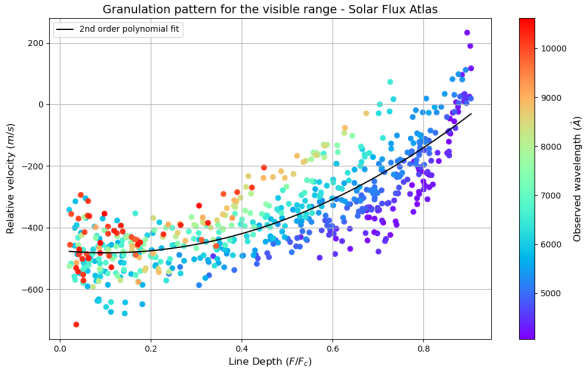

Figure 4.9: We realized the same graphic for the comparision with the Ellwarth article to show the less scattered points.

Chapter 5

Conclusions

In general, we conclude... Characterize the convective blueshift of solar absorption lines and its dependence on line depth and wavelength range.

In specific, we produce a blend-free list of Fe I absorption lines and solar granulation patterns with minimal scatter. We describe in detail how the granulation plot depends on wavelength range. We explore possible explanations of wavelength-dependence and found thats () is the best. We explore ways of dealing with the wavelength-dependence when using the solar spectrum as a gauge for stellar spectra.

Appendix A

Z-score Standardization

This was for a problem present in the fit and we just use a acomputational stadarization in the selected bins of fits to make a standarization.

Appendix B

The third derivate relation

Or called the bisector slope. It was multiplied by the relation $(\frac{c}{\lambda})$ to see each clear in the graphic.

Appendix C

Visualizer for outliers

Was an app made with Tkinter for help the visualization of outliers in the process of blendfree the Fe I list. There is in the Git hub

Bibliography

[1] S. A. Hamouda, F. F. Alfarjani, and F. Y. Elfituri, "Sunspots production and relation to other phenomena: A review," *International Journal of Science and Research Methodology*, 06 2018.

[2] T. A. Nieminen, "Solar line asymmetries: Modelling the effect of granulation on the solar spectrum," *arXiv*, Aug. 2017. arXiv:1708.06408 [astro-ph].

[3] D. F. Gray, "The third signature of stelar granulation," *The Astrophysical Journal*, vol. 697, p. 1032, May 2009.

[4] D. Dravins, L. Lindegren, and A. Nordlund, "Solar granulation - influence of convection on spectral line asymmetries and wavelength shifts," *Astronomy and Astrophysics*, vol. 96, p. 345–364, Mar. 1981.

[5] D. Hamilton and J. B. Lester, "A technique for the study of stellar convection: The visible solar flux spectrum," *Publications of the Astronomical Society of the Pacific*, vol. 111, p. 1132, Sept. 1999.

[6] A. Reiners, N. Mrotzek, U. Lemke, J. Hinrichs, and K. Reinsch, "The iag solar flux atlas: Accurate wavelengths and absolute convective blueshift in standard solar spectra," *Astronomy and Astrophysics*, vol. 587, p. A65, Mar. 2016.

[7] F. Peter, *Solar Astrophysics*. Cambridge research and instrumentation, 1990.

[8] D. F. Gray and T. Pugh, "The third signature of granulation in bright-giant and supergiant stars," *The Astronomical Journal*, vol. 143, p. 92, Mar. 2012.

[9] M. Ellwarth, B. Ehmann, S. Schäfer, and A. Reiners, "Convective characteristics of fe i lines across the solar disc," *Astronomy and Astrophysics*, vol. 680, p. A62, Dec. 2023.

[10] G. Nave, S. Johansson, R. C. M. Learner, A. P. Thorne, and J. W. Brault, "A new multiplet table for fe i," *The Astrophysical Journal Supplement Series*, vol. 94, p. 221, Sept. 1994.

[11] A. Cacciani, R. Briguglio, F. Massa, and P. Rapex, "Precise measurement of the solar gravitational red shift," *Celestial Mechanics and Dynamical Astronomy*, vol. 95, p. 425–437, May 2006.

[12] P. Eric, *Solar magnetohydrodynamics*. Kluwer, 1982.

[13] B. Carroll and D. Ostlie, *An Introduction to Modern Astrophysics*. Cambridge University Press, 2017.

[14] B. Ryden, *Introduction to cosmology*. Cambridge University Press, 2016.

[15] D. F. Gray and B. Oostra, "The solar-flux third granulation signature," *The Astrophysical Journal*, vol. 852, p. 42, Jan. 2018. ADS Bibcode: 2018ApJ...852...42G.

[16] J. S. Aponte, "Medición de la velocidad convectiva en la fotosfera solar," 2017.

[17] F. Stief, J. Löhner-Böttcher, W. Schmidt, T. Steinmetz, and R. Holzwarth, "Convective blueshifts in the solar atmosphere - ii. high-accuracy observations of the fe i 6173.3 Å line and deviations of full-disk dopplergrams," *Astronomy & Astrophysics*, vol. 622, p. A34, Feb. 2019.